Advances in Nano Research, *Vol. 10, No. 1 (2021) 71-76*
DOI: https://doi.org/10.12989/anr.2021.10.1.071

Qualitative comparison of chemical and green synthesized Fe_3O_4 nanoparticles

V. Gokila[a], V.T. Perarasu* and R. Delma Jones Rufina[b]

Thermal and Bio Analysis Laboratory, Department of Chemical Engineering, AC Tech Campus, Anna University, Chennai 600025, Tamil Nadu, India

(*Received January 31, 2020, Revised October 28, 2020, Accepted November 4, 2020*)

Abstract. Synthesis of nanoparticles using green technology using plants is gaining significant attention as it is an environmentally friendly substitute to conventional physical and chemical methods. The present study was focused on the chemical and green synthesis of Iron Oxide nanoparticles from ferric chloride. The green synthesis was achieved by utilizing the bio components of *Hibiscus rosa-sinensis.* The Fe_3O_4 nanoparticles with the size range of 87-400 nm were synthesized by wet chemical reduction technique which are unstable, prone to aggregation while in green synthesis the phytochemicals present in the leaf extract acts as the capping as well as the reducing agent thus the green synthesized iron (III) oxide nanoparticles were naturally stabilized, spherical shaped and are in the size range of 2-80 nm. The results of both the protocols are compared and presented briefly.

Keywords: chemical synthesis; Fe_3O_4 nanoparticles; green synthesis; phytochemicals

1. Introduction

Nanotechnology is sizzling in wide range of applications in recent times due to its unique properties of nanomaterials at nanoscale (Nasrollahzadeh *et al*. 2019). The optical, magnetic, electrical and various other properties either emerge freshly or exhibit in new form from the existing ones (Pugazhendhi *et al*. 2018). This kindles the researcher's interest to explore the nanotechnology in all possible ways. The field of nanotechnology takes in the construction and utilization of physical, chemical and biological systems with nano structural features between single atoms or molecules to submicron dimensions. In precise, manipulation of materials at nano-scale (Muthukumar *et al*. 2019, Nasrollahzadeh *et al*. 2019).

Synthesis of nanomaterials extensively falls under two categories: Top-down approach and bottom-up approach. Top-down approach implicates in achieving nano-scale from bulk whereas the bottom-up approach involves in chemical reactions of molecules to get nano materials. Conventional chemical synthesis and recent bio synthesis falls under bottom-up approach.

The chemical and physical synthesis involve use of expensive and toxic chemicals as capping and reducing agents. The use of hazardous and toxic chemical will cause adverse effect in application side (Chaki *et al*. 2015). Chemical synthesis involves in reducing the precursor solution using any mild or strong reducing agent. In this method, the capping agent should be used in particular to prevent the agglomeration of particles for better results.

Green synthesis is an emerging area in the field of bio nanotechnology as an alternative to chemical and physical methods (Pugazhendhi *et al*. 2018, Thunugunta and Reddy 2015, Wang *et al*. 2019). Biosynthesis or green synthesis of nanoparticles is a kind of scale down or bottom up approach in which the main reaction occurring is reduction or oxidation. The phytochemicals (polyphenols, reducing sugars, nitrogenous bases, amino acids, etc.) are usually responsible for reduction of metal compounds to their corresponding nanoparticles (Mohanpuria *et al*. 2008). In this green approach, nontoxic safe reagents which are eco-friendly and bio safe are used (Mohanpuria *et al*. 2008, Zhu *et al*. 2019). Naturally available compounds or micro-organisms or plant extracts are used as the reducing agents. The use of plant extracts in the green synthesis of metal oxide nanoparticles has drawn a considerable attention as it is a straightforward approach (Abdul Salam *et al*. 2014, Kanagasubbulakshmi and Kadirvelu 2017). Many recent and on-going research uses plant extract for synthesis of metal nanoparticles and metal-oxide nanoparticles.

Both green and chemical synthesis have their own pros and cons. Few to be highlighted are the metal oxides prepared by green synthesis are more stable than that of its opponent but while comparing the yield, the chemical synthesis ranks better (Chaki *et al*. 2015). The major positive aspect of green synthesis is mainly the plant extract itself stabilises the resultant nanoparticles. Separate capping agent is not needed (Muthukumar *et al*. 2019, Pugazhendhi *et al*. 2018, Wang *et al*. 2019). Also, green paves simple and very easy methodology to attain nanoparticles compared to

*Corresponding author, Associate Professor,
E-mail: vtparasu@annauniv.edu
[a] M.Tech. Student,
E-mail: gokilavenkatarathinam@gmail.com
[b] Ph.D. Student, E-mail: joh.commutech@gmail.com

ISSN: 2287-237X (Print), 2287-2388 (Online)

that of chemical synthesis (Iravani 2011, Kharissova *et al*. 2013, Muthukumar *et al*. 2019, Pugazhendhi *et al*. 2018, Wang *et al*. 2019).

Iron oxide nanoparticles (Fe_3O_4 NPs) have variety of applications like catalyst, adsorption of heavy metals, antibiotic degradations. In particular its anti-microbial activity drives more interest (Makarov *et al*. 2014, Vasantharaj *et al*. 2019).

Hibiscus rosa-sinensis (HR) is the plant of interest for our green synthesis (Al-Snafi 2018, Devi and Gayathri 2014, Reveendran *et al*. 2016, Yardily and Sunitha 2019). It is an ornamental plant which is readily available in abundance. Researchers have used various plant in preparing metal nanoparticles and metal oxide nanoparticles (Kanagasubbulakshmi and Kadirvelu 2017, Makarov *et al*. 2014, Njagi *et al*. 2011, Vasantharaj *et al*. 2019). *Hibiscus rosa-sinensis* have been chosen in this work, since it is easily available. Leaves were selected as it has higher polyphenolic content and low molecular weight organic acid content. On the other hand, for chemical synthesis, wet chemical method was used. In this method, the precursor ferric chloride was reduced using sodium borohydride.

In this work, iron oxide nanoparticles were prepared through chemical synthesis as well as green synthesis. It is intended to investigate the features of nanoparticles through both the means. The comparative analyses of as-prepared iron oxide nanoparticles by both green and chemical syntheses are presented.

2. Materials and methods

2.1 Experimental procedure

Chemicals and solvents were purchased from sigma Aldrich chemical company. All chemicals and solvents were of analytical grade and they were used as purchased without any further purification. The detailed explanations of the protocols are as follows.

2.1.1 Chemical synthesis of NPs

The Fe_3O_4 nanoparticles were synthesized by simple wet chemical reduction technique. 10 ml of 2.5M sodium borohydride ($NaBH_4$) solution was prepared in a 100 ml clean glass dry beaker under magnetic stirring. Then 40 ml 0.1M ferric chloride hexa-hydrate ($FeCl_3 \cdot 6H_2O$) solution was prepared and added drop wise in to the sodium hydroxide solution under vigorous stirring. With gradual addition of ferric chloride the solution became darker and eventually became complete black. Fe_3O_4 nanoparticles were produced in black precipitates. The Fe_3O_4 nanoparticles were filtered and washed with distilled water and absolute methanol for several times and then the particles were dried in oven for overnight at 50°C. The possible chemical reaction for this method is based on the Fe^{3+} ions reduction using sodium borohydride ($NaBH_4$) as reducing agent according to the following reaction (Ruíz-Baltazar *et al*. 2015).

$$4Fe_{(aq)}^{3+} + 3BH_{4(aq)}^{-} + 9H_2O \rightarrow 4Fe_{(s)}^{0} + 3H_2BO_{3(aq)}^{-} + 12H_{(aq)}^{-} + 6H_{2(g)}$$

2.1.2 Green synthesis of NPs

Freshly collected leaves from *Hibiscus rosa-sinensis* were collected, dried and grounded. For the preparation of extract, powdered HR leaves were heated. The solution was filtered and the filtrate obtained was stored at −4°C for future use. This extract acts as a reducing agent as well as capping agent for the synthesis of nanoparticles.

Iron oxide NPs were synthesized by adding $FeCl_3$ and HR leaves extract in 1:1 volume ratio. Iron oxide NPs were immediately obtained with the reduction process. The formation of iron oxide NPs was found by appearance of dark brown colour. HR leaves have the best reduction capability against ferric chloride when compared to other parts of the plants

2.2 Instrumentation

2.2.1 UV – Visible spectroscopy

UV-Visible spectroscopy (UV-Vis) is a powerful analytical technique used to determine the optical properties of liquid samples. UV-Visible spectrophotometer (UV-1800) is an advanced high-resolution spectrophotometer used to measure the absorbance of the samples in the wavelength range of 190 to 1100 nm.

2.2.2 Particle size analysis

Particle size analysis is used to characterize the size distribution of particles in a given sample. The Nano Plus, Micromeritics instrument measures the particle size of samples suspended in liquids (dilution method) in the range of 0.1 nm to 12.3 μm with sample suspension concentrations from 0.00001 to 40% and a sensitivity for molecular weight to as low as 250 Da. The study was made at the temperature of 25°C and the intensity of the radiation is kept at 31948 (cps). The diameter of the particle was obtained from the Stokes-Einstein equation

$$D = \frac{nKT}{3\pi\eta d} \quad (1)$$

where d is the diameter of the NPs, D is the diffusion coefficient, K is the Boltzman constant (1.3807×10^{-23} $J.K^{-1}$), T is the temperature, and η is the viscosities of the medium. The Polydispersity Index (PDI) is the size distribution of the nanoparticle population which was calculated using the formula.

$$PDI = \left[\frac{\text{Standard deviation}}{\text{Average diameter}}\right]^2 \quad (2)$$

2.2.3 X-ray diffraction analysis

X- ray diffractometer (PANalytical X'pert powder XRD system), operating in transmission mode is used to analyse the presence of synthesized NPs. This instrument uses a Cu lamp as radiation source (λ = 1.54056 Å at 45 kV and 30 mA), in the range of 30 to 75°, with step size of 0.0200° and scan time of 1 s for each step. Continuous type scanning was used. Gonio scan axis was used to analyse the sample. The average crystallite size was calculated from the X-Ray Diffraction analysis (XRD) data using Scherrer's equation

$$D = \frac{K\lambda}{\beta cos\theta} \quad (3)$$

where D is particle size, k is the grain shape factor taken as unity contemplating that the particles are spherical in shape, λ is the incident x-ray wavelength of Cu-Kα radiation and θ is the Bragg's angle, β is the broadening of diffraction line measured at half maximum intensity (radians).

2.2.4 Fourier transform – infrared spectroscopy analysis

Fourier Transform-Infrared Spectroscopy Analysis (FT-IR) is a fascinating technique to evaluate structural variations on samples due to the chemical treatments. FT-IR spectrum two perkin elmer instrument was used to identify the compounds that are present in the synthesized NPs. The spectra were collected in the range of 4000 to 400 cm^{-1}, with a resolution of 4 cm^{-1} and 64 scans per sample.

2.2.5 Scanning electron microscopy analysis

A Scanning Electron Microscope (SEM) is a type of electron microscope that focus a high energy electron beam over a surface of the sample to create an image. Gold-sputtered samples were observed at an accelerating voltage of 5 kV with a magnification of 500 and working distance of 11700 µm and emission current of 70000 nA.

3. Results and discussions

3.1 UV – visible spectroscopy

The preliminary characterisations for the synthesized Fe_3O_4 NPs were made using UV-Visible spectroscopy. The obtained Fe_3O_4 NPs were sonicated to get clear colloidal solution. This was dispersed in distilled water and was used as a sample and distilled water was used as reference. Once the reducing agent was added, the absorption peak of the ferric (III) chloride (419 nm) was shifted to 311 nm which indicates the formation of Fe_3O_4 NPs. This narrow peak with the absorbance of 3.331 is due to increase in number of NPs formed as a result of reduction of ferric chloride ions.

The Fig. 1(a) shows the absorbance spectrum of the chemically synthesized Fe_3O_4 NPs at ambient temperature. The absorption edge lies between 270 and 300 nm for the synthesized NPs. This absorption spectrum correlated and are in good accordance with

The Fig. 1(b) shows the optical absorbance spectrum of varying concentration of green synthesized Fe_3O_4 NPs at ambient temperature. The colloidal solution of Fe_3O_4 NPs was used as a sample and distilled water was used as reference.

The phytochemicals present in the plant extract acts as the effective metal-reducing agents and as capping agents which provides coating over the metal NPs in a single step and causes colour change from yellowish brown to brownish black indicating the formation of iron-containing NPs.

This change correlated well with the absorption spectra data, such that the absorption peak at 669 nm clearly

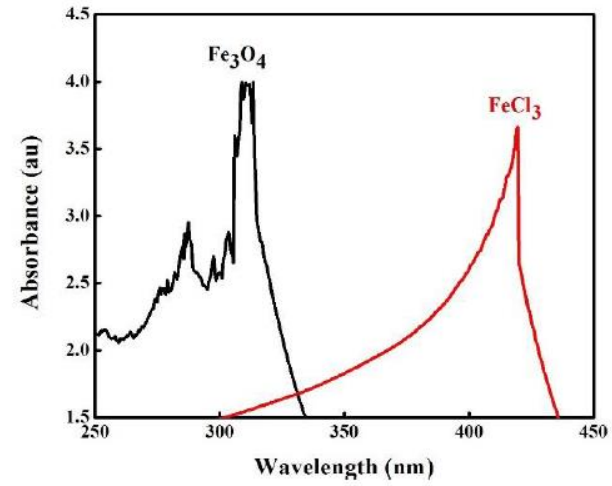

(a) Chemical

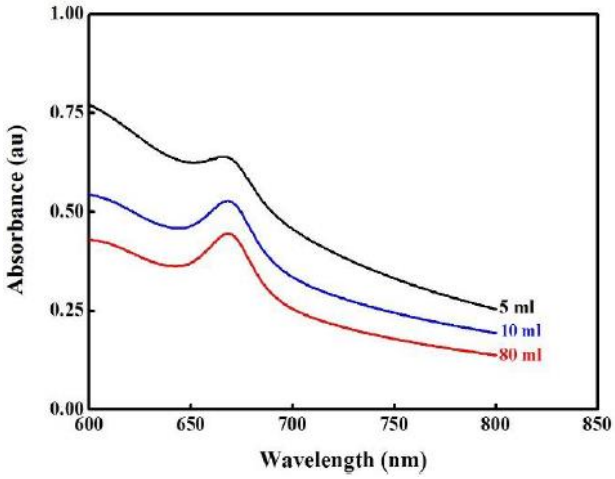

(b) Green

Fig. 1 UV-Vis spectrum of Fe_3O_4 NPs

indicates the addition of the of the plant extracts to the ferric (III) chloride with the absorbance of 0.531 being indicative of the formation of iron (III) oxide NPs. The absorption edge lies between 650 and 700 nm for the synthesized NPs.

3.2 Particle size analysis

The preliminary size characterisation of the synthesized NPs was studied by using particle size analyser. The average size of the chemically synthesized NPs was in the range of 87-400 nm with the average diameter of about 158.3 nm.

The Fig. 2(a) shows the particle size analysis of the chemically synthesized Fe_3O_4 NPs.

The diameter of the chemical and green synthesized NPs was found to be 167.7 nm and 3.1 nm respectively using the Stokes-Einstein equation. The PDI and scattering intensity of chemically synthesized NPs were found to be 0.331 and 33021 cps respectively.

The Fig. 2(b) shows the particle size analysis of the green synthesized Fe_3O_4 NPs. The average size of the NPs was in the range of 2-80 nm which shows the well size

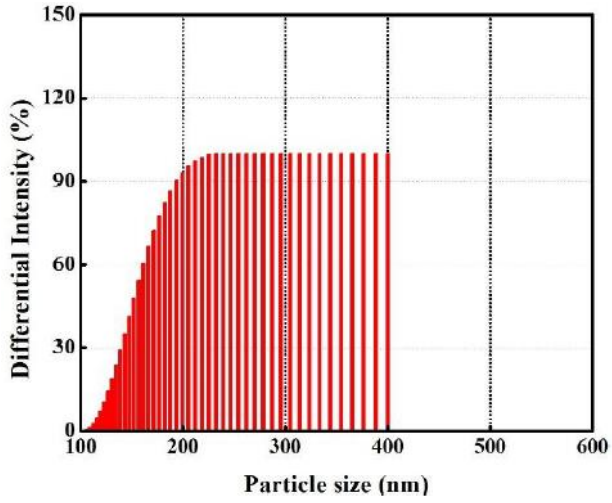

(a) Chemical

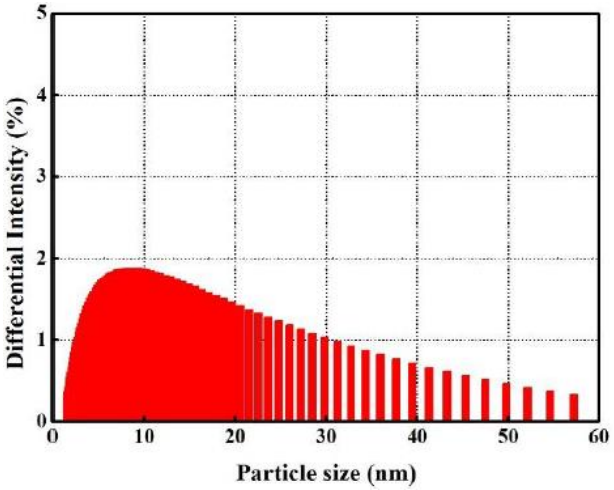

(b) Green

Fig. 2 Particle size analysis of Fe_3O_4 NPs

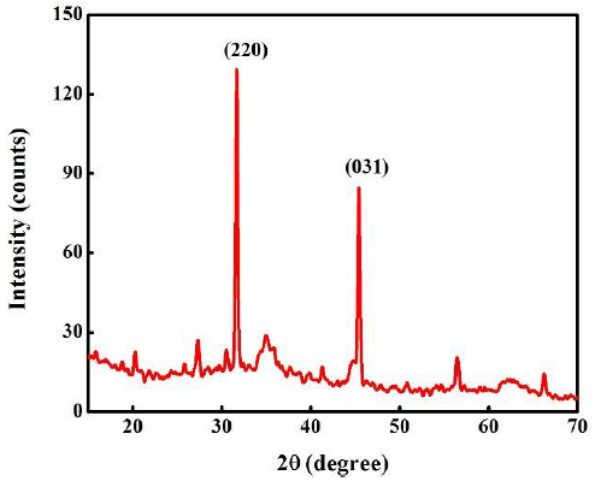

(a) Chemical

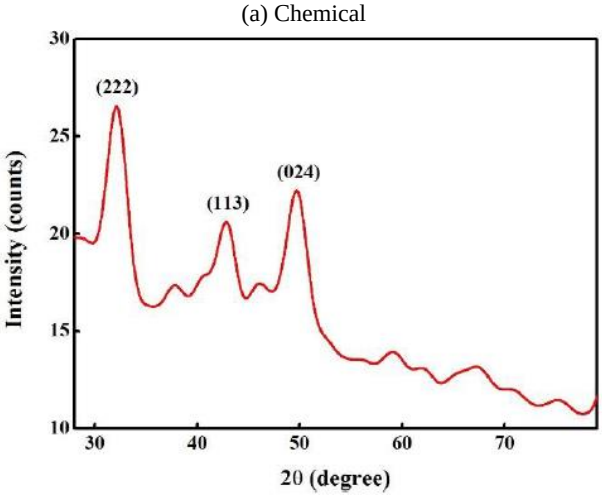

(b) Green

Fig. 3 XRD pattern of Fe_3O_4 NPs

reduction by plant extract with the average diameter of about 12.9 nm. The PDI and scattering intensity of green synthesized NPs were found to be 0.002 and 28319 cps respectively. Higher PDI value of chemically synthesized NPs indicates that the particles were polydisperse and non-uniform in nature. These particles were unstable in comparison with the green NPs.

3.3 X-ray diffraction analysis

Fig. 3(a) shows the X-ray diffraction for the chemically synthesized NPs.

Fig. 3(a) reveals the diffraction peaks at 2θ = 31.64° with a crystallographic plane (220) and 45.633° with a crystallographic plane (031) which corresponds to Fe_3O_4 NPs. The XRD did not show any other phases such as FeO, Fe_2O_3, etc. The Fig. 3(b) shows the X-ray diffraction for the synthesized NPs using the HR leaves extract.

The XRD pattern with the strong diffraction peaks with 2θ values of 32.28°, 40.63°, 49.72° corresponding to the hkl values of (222), (113), (024) corresponds to crystalline phase of Fe_3O_4 NPs, respectively.

This peak value matches with JCPDS card No. 39-1346 and JCPDS card No. 89-4319 for iron (III) oxide NPs. The average crystallite size came out to be 82.23 nm and 19 nm for chemical and green synthesized NPs respectively using Scherrer's equation. This clearly indicates that the particles were agglomerated and was unstable in case of chemical synthesis.

3.4 Fourier transform – infrared spectroscopy analysis

FT-IR spectrum of dispersed chemically synthesized Fe_3O_4 NPs in distilled water is shown in the Fig. 4(a).

FT- IR analysis gave the peak at 3448.52 cm^{-1} which was due to –OH stretching vibration arising from hydroxyl groups from the distilled water used as the solvent for the synthesis of NPs. The absorption peaks at 2927.26 cm^{-1}, 1636.78 cm^{-1}, 1384.42 cm^{-1} and 1021.00 cm^{-1} were due to C=O vibrations which indicated that reducing agent molecules were chemically bonded to the surface of Fe_3O_4 NPs. The 672.35 cm^{-1}, 557.71 cm^{-1} and 503.27 cm^{-1} absorption peaks correspond to the Fe-O bond vibration of Fe_3O_4 NPs.

FT- IR analysis gave the stretching vibrations at 3436.27 cm^{-1}, 2075.03 cm^{-1}, 1634.52 cm^{-1} and 706.84 cm^{-1} with in

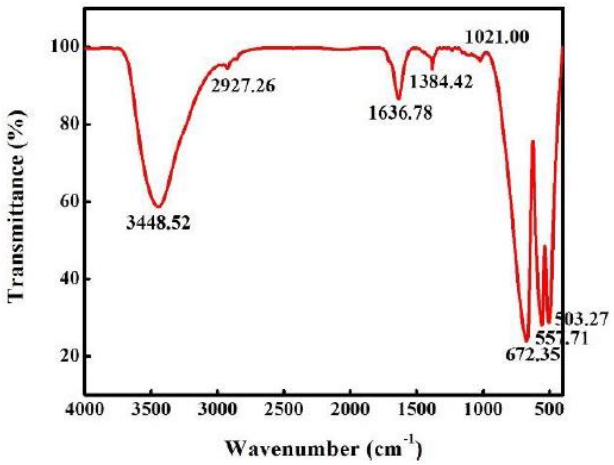

(a) Chemical

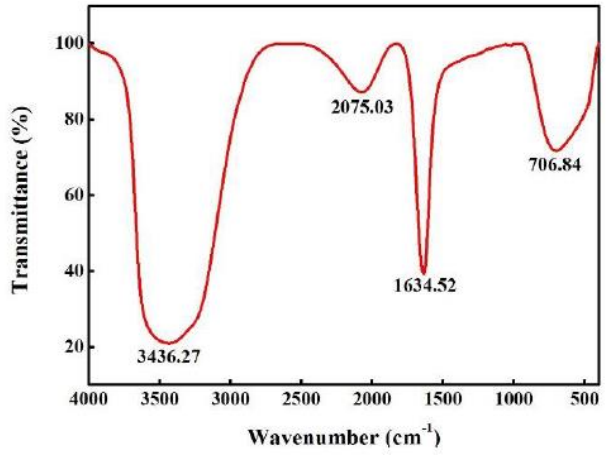

(b) Green

Fig. 4 FT- IR Spectrum of Fe_3O_4 NPs

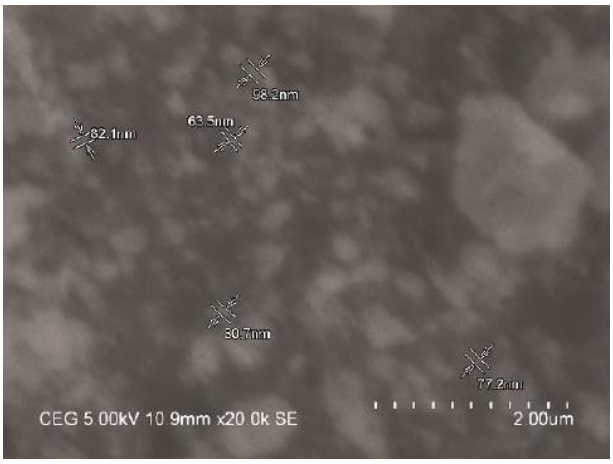

(a) Chemical

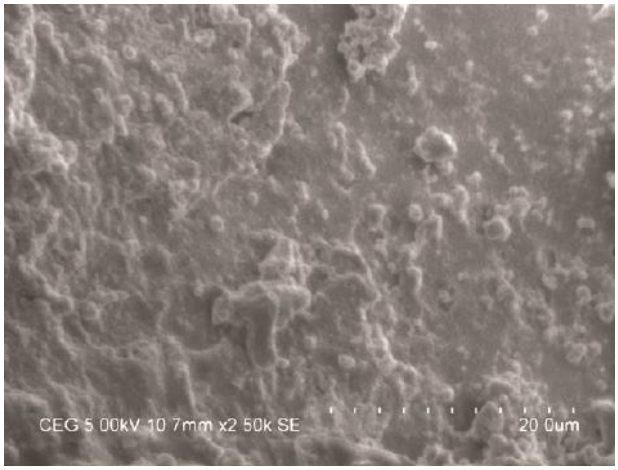

(b) Green

Fig. 5 SEM analysis for Fe_3O_4 NPs

the region of 400-4000 cm^{-1} for the green synthesized NPs. FT-IR spectrum of synthesized Fe_3O_4 NPs in plant extract is shown in the Fig. 4(b).

These peaks represent the following bonding in the sample confirms the reducing agent role in the formation of Fe_3O_4 NPs. The stretching vibrations at 3436.27 cm^{-1} corresponds to the -OH bond stretching denotes the aqueous phase as well as the reduction of the ferric (III) chloride, the phytochemicals present in the plant extract and amino acids which stabilise as well as act as a capping agents was proved by the absorption peak at around 2075.03 cm^{-1} and 1634.52 cm^{-1} corresponds to the C=O bond stretching and the less intense narrow peak at 706.84 cm^{-1} corresponds to the inorganic stretching indicates the Fe_3O_4 NPs. These functional groups were believed to facilitate formation of iron (III) oxide NPs.

3.5 Scanning electron microscopy analysis

SEM reveals the surface topography of the synthesized Fe_3O_4 NPs. The SEM images of the chemically synthesized Fe_3O_4 NPs are given below (Fig. 5(a))

This showed the highly irregular shaped Fe_3O_4 NPs due to the agglomeration of the particles. The particles were irregular shaped with the varying sizes. This result was in good accordance with SEM analysis of green Fe_3O_4 NPs is shown below Fig. 5(b). SEM image has showed individual iron (III) oxide particles as well as a number of aggregates. It showed the relatively spherical shaped nanoparticle.

4. Conclusions

In this study, Iron oxide nanoparticles were synthesized using green and chemical protocols, and their comparative studies have been done using various characterization. Initial investigation was done using UV-VIS spectroscopy. FT-IR, XRD was done to investigate the structure of nanoparticles. The size of the particles was characterised using particle size analyser and SEM. The particle size of Fe_3O_4 NPs was found to be in the range of 87-400 nm and 2-80 nm for chemical and green synthesis respectively. Also, higher PDI (0.331) indicates the non-uniformity in size. On the other hand, NPs were stabilized more naturally using plant extracts that are known to contain high concentrations of low molecular weight organic acids. These acids formed the coating over the particles and prevented them from aggregating. The lower value of PDI (0.002) for the green synthesized NPs indicates the uniform size of the particles.

References

Al-Snafi, A.E. (2018), "Chemical constituents, pharmacological effects and therapeutic importance of *Hibiscus rosa-sinensis* - A review", *J. Pharm.*, **8**(7), 101-119.

Chaki, S.H., Malek, T.J., Chaudhary, M.D., Tailor, J.P. and Deshpande, M.P. (2015), "Magnetite Fe_3O_4 nanoparticles synthesis by wet chemical reduction and their characterization", *Adv. Nat. Sci. Nanosci. Nanotechnol.*, **6**(3), 035009. http://dx.doi.org/10.1088/2043-6262/6/3/035009.

Devi, R.S. and Gayathri, R. (2014), "Green synthesis of zinc oxide nanoparticles by using *Hibiscus rosa-sinensis*", *Int. J. Curr. Eng. Technol.*, **4**(4), 2444-2446.

Iravani, S. (2011), "Green synthesis of metal nanoparticles using plants", *Green Chem.*, **13**(10), 2638-2650. http://dx.doi.org/10.1039/C1GC15386B.

Kanagasubbulakshmi, S. and Kadirvelu, K. (2017), "Green synthesis of iron oxide nanoparticles using *Lagenaria siceraria* and evaluation of its antimicrobial activity", *Defence Life Sci. J.*, **2**(4), 422-427. https://doi.org/10.14429/dlsj.2.12277.

Kharissova, O.V., Dias, H.R., Kharisov, B.I., Perez, B.O. and Perez, V.M.J. (2013), "The greener synthesis of nanoparticles", *Trends Biotechnol.* **31**(4), 240-248. https://doi.org/10.1016/j.tibtech.2013.01.003.

Makarov, V.V., Makarova, S.S., Love, A.J., Sinitsyna, O.V., Dudnik, A.O., Yaminsky, I.V., Taliansky, M.E. and Kalinina, N.O. (2014), "Biosynthesis of stable iron oxide nanoparticles in aqueous extracts of *Hordeum vulgare* and *Rumex acetosa* plants", *Langmuir*, **30**(20), 5982-5988. https://doi.org/10.1021/la5011924.

Mohanpuria, P., Rana, N.K. and Yadav, S.K. (2008), "Biosynthesis of nanoparticles: Technological concepts and future applications", *J. Nanopart. Res.*, **10**(3), 507-517. https://doi.org/10.1007/s11051-007-9275-x.

Muthukumar, H., Mohammed, S.N., Chandrasekaran, N., Sekar, A.D., Pugazhendhi, A. and Matheswaran, M. (2019), "Effect of iron doped Zinc oxide nanoparticles coating in the anode on current generation in microbial electrochemical cells", *Int. J. Hydrog. Energy*, **44**(4), 2407-2416. https://doi.org/10.1016/j.ijhydene.2018.06.046.

Nasrollahzadeh, M., Sajadi, S. M., Sajjadi, M. and Issaabadi, Z. (2019), "An introduction to nanotechnology", *Interf. Sci. Technol.*, **28**, 1-27. http://dx.doi.org/10.1016/B978-0-12-813586-0.00001-8.

Njagi, E.C., Huang, H., Stafford, L., Genuino, H., Galindo, H.M., Collins, J.B., Hoag, G.E. and Suib, S.L. (2010), "Biosynthesis of iron and silver nanoparticles at room temperature using aqueous sorghum bran extracts", *Langmuir*, **27**(1), 264-271. https://doi.org/10.1021/la103190n.

Pugazhendhi, A., Kumar, S.S., Manikandan, M. and Saravanan, M. (2018), "Photocatalytic properties and antimicrobial efficacy of Fe doped CuO nanoparticles against the pathogenic bacteria and fungi", *Microb. Pathog.*, **122**, 84-89. https://doi.org/10.1016/j.micpath.2018.06.016.

Reveendran, A., Varghese, S. and Viswanathan, K. (2016), "Green synthesis of silver nano particle using *Hibiscus rosa-sinensis*", *IOSR J. Appl. Phys.*, **8**, 35-38. https://doi.org/10.9790/4861-0803023538.

Ruíz-Baltazar, A., Esparza, R., Rosas, G. and Pérez, R. (2015), "Effect of the surfactant on the growth and oxidation of iron nanoparticles", *J. Nanomater.*, **2015**, 240948. https://doi.org/10.1155/2015/240948.

Salam, H.A., Sivaraj, R. and Venckatesh, R. (2014), "Green synthesis and characterization of zinc oxide nanoparticles from *Ocimum basilicum L. var. purpurascens Benth- Lamiaceae* leaf extract", *Mater. Lett.*, **131**, 16-18. https://doi.org/10.1016/j.matlet.2014.05.033.

Thunugunta, T. and Reddy, A.C. (2015), "Green synthesis of nanoparticles: Current prospectus", *Nanotechnol. Rev.*, **4**(4), 303-323. https://doi.org/10.1515/ntrev-2015-0023.

Vasantharaj, S., Sathiyavimal, S., Senthilkumar, P., LewisOscar, F. and Pugazhendhi, A. (2019), "Biosynthesis of iron oxide nanoparticles using leaf extract of Ruellia tuberosa: Antimicrobial properties and their applications in photocatalytic degradation", *J. Photochem. Photobiol. B Biol.*, **192**, 74-82. https://doi.org/10.1016/j.jphotobiol.2018.12.025.

Sarsar, V., Selwal, K.K. and Selwal, M.K. (2014), "Nanosilver: Potent antimicrobial agent and its biosynthesis", *Afr. J. Biotechnol.*, **13**(4), 546-554. https://doi.org/10.5897/AJB2013.13147

Wang, Y., O'Connor, D., Shen, Z., Lo, I.M., Tsang, D.C, Pehkonen, S., Pu, S. and Hou, D. (2019), "Green synthesis of nanoparticles for the remediation of contaminated waters and soils: Constituents, synthesizing methods and influencing factors", *J. Clean. Prod.*, **226**, 540-549. https://doi.org/10.1016/j.jclepro.2019.04.128.

Yardily, A. and Sunitha, N. (2019), "Green synthesis of iron nanoparticles using hibiscus leaf extract, characterization, antimicrobial activity", *Int. J. Sci. Res. Rev.*, **8**, 32-46.

Zhu, X., Pathakoti, K. and Hwang, H.M. (2019), *Green Synthesis, Characterization and Applications of Nanoparticles*, Elsevier, Amsterdam, Netherlands. https://doi.org/10.1016/B978-0-08-102579-6.00010-1

CC